Efficient CRISPR-Cas9-mediated mutagenesis in primary human B cells for identifying plasma cell regulators

Tuan Anh Le,[1,2] Van Trung Chu,[3] Andreia C. Lino,[1,2] Eva Schrezenmeier,[4,5] Christopher Kressler,[1,6] Dania Hamo,[1,6] Klaus Rajewsky,[3] Thomas Dörner,[1,2,8] and Van Duc Dang[1,2,7,8]

[1]Deutsches Rheuma-Forschungszentrum, A Leibniz Institute, Charitéplatz 1, 10117 Berlin, Germany; [2]Department of Rheumatology and Clinical Immunology, Charité-Universitätsmedizin Berlin, Berlin, Germany; [3]Max-Delbrück-Center for Molecular Medicine in the Helmholtz Association (MDC), Immune Regulation and Cancer, 13125 Berlin, Germany; [4]Department of Nephrology and Medical Intensive Care, Charité-Universitätsmedizin Berlin, Corporate Member of Freie Universität Berlin, and Humboldt-Universität zu Berlin, Berlin, Germany; [5]Berlin Institute of Health (BIH), Berlin, Germany; [6]Berlin Institute of Health Center for Regenerative Therapies (BCRT), Charité - Universitätsmedizin Berlin, Berlin, Germany; [7]Faculty of Biology, VNU University of Science, Vietnam National University, Hanoi, Vietnam

Human B lymphocytes are attractive targets for immunotherapies in autoantibody-mediated diseases. Gene editing technologies could provide a powerful tool to determine gene regulatory networks regulating B cell differentiation into plasma cells, and identify novel therapeutic targets for prevention and treatment of autoimmune disorders. Here, we describe a new approach that uses CRISPR-Cas9 technology to target genes in primary human B cells in vitro for identifying plasma cell regulators. We found that sgRNA and Cas9 components can be efficiently delivered into primary human B cells through RD114-pseudotyped retroviral vectors. Using this system, we achieved approximately 80% of gene knockout efficiency. We disrupted expression of a triad of transcription factors, IRF4, PRDM1, and XBP1, and showed that human B cell survival and plasma cell differentiation are severely impaired. Specifically, that IRF4, PRDM1, and XBP1 were expressed at different stages during plasma cell differentiation, IRF4, PRDM1, and XBP1-targeted B cells failed to progress to the pre-plasmablast, plasma cell state, and plasma cell survival, respectively. Our method opens a new avenue to study gene functions in primary human B cells and identify novel plasma cell regulators for therapeutic applications.

INTRODUCTION

Plasma cells (PCs) are known for their unique ability to secrete antibodies, which is the basis of humoral immunity. Recent studies in mice have shown that PCs can also regulate immunity through production of anti-inflammatory cytokines such as interleukin (IL)-10 and IL-35.[1–4] Distinct PC subsets with protective and pathogenic functions have been identified by the expression of certain surface markers in both mouse and humans,[1,3,5,6] providing possible selective depletion approaches of the pathogenic cells in various diseases. Nevertheless, this strategy is limited as those surface markers are also expressed by other immune cell lineages. Alternatively, key transcription factors (TFs) or/and intracellular regulators, which are

essential for the generation of pathogenic PCs, hold promise as potential therapeutic targets. Such strategies have been developed for targeting TFs controlling T cell immunity in pre-clinical mouse models as well as clinical trials for autoimmune and malignant diseases.[7–9] To date, a triad of TFs, IRF4, BLIMP1, and XBP1, has been identified as key regulators of mouse PC differentiation,[10–13] meanwhile, the relevant molecules are poorly described in human PCs. In addition, molecular pathways regulating differentiation, survival, and antibody production of human PCs remain incompletely understood.

CRISPR-Cas9-mediated targeted mutagenesis can be harnessed for deciphering the gene regulatory networks governing PC differentiation. In mice, the CRISPR-Cas9 system has been successfully established to identify PC regulators in primary B cells isolated from Cas9 transgenic mice.[13] Apart from that, several attempts have been undertaken to use CRISPR-Cas9 in studies of human B cell biology.[14–16] Unlike Cas9-expressing mouse B cells requiring only single guide RNA (sgRNA) presence,[13] gene editing of primary human B cells only happens when both sgRNA and Cas9 protein are present in the target cells. Synthetic sgRNAs and Cas9 protein can be delivered into primary human B cells as ribonucleoprotein (RNP) complexes using electroporation.[17] However, this approach shows limitations in attempts to track the gene-edited cells or perform large-scale screening because of the lack of reporters and substantial costs, respectively. In contrast, the delivery of sgRNA and Cas9 by virus-based system could overcome those limitations.[18] The biggest

hurdle of viral approaches is the large coding sequence of Cas9, which results in low infectious virus titers.[19] Recently, Caeser et al. reported the delivery of Cas9 into primary human germinal center B cells isolated from tonsil tissue using Gibbon Ape Leukemia Virus (GaLV)-pseudotyped viruses.[18] However, in this system, human germinal center B cells were transduced with Cas9 and oncogenic BCL2-BCL6 vectors, and followed by additional transduction with Cas9 vectors to reach an adequate transduction efficiency. Therefore, experimental workflows that allow efficient delivery of CRISPR-Cas9 for primary human B cells and the study of molecules governing human B cell activation, B cell differentiation and antibody secretion are still needed.

Here, we developed a method that efficiently delivers Cas9 and sgRNA into primary human B cells using RD114-pseudotyped retroviral vectors with a gene knockout efficiency of approximately 80%. Remarkably, using this method, we showed that knockout of *IRF4*, *PRDM1*, and *XBP1* leads to a marked abrogation of human PC differentiation from naive B cells. Collectively, we establish a robust and reliable method to efficiently screen for regulators controlling PC differentiation.

RESULTS
Efficient transduction of primary human B cells with RD114-pseudotyped retroviral vector
It has been shown that human hematopoietic stem and T cells are susceptible to RD114-pseudotyped retroviral vectors.[20] To test whether primary human B cells are also susceptible to RD114-pseudotyped retroviral vectors, we produced these particles using 293Vec-RD114 cell line that stably and highly expresses retroviral structure proteins (gag, pol, and RD114 envelope). As controls, we included amphotropic and GaLV-pseudotyped retroviral vectors produced from Platinum-A and 293Vec-GaLV cell lines, respectively. Another GaLV-pseudotyped retroviral vector was produced from HEK-293T cell line by co-transfecting packaging (pHIT60) and envelope (GaLV WT) plasmids. All retroviral vectors were produced with the same main sgRNA plasmid harboring mCherry reporter (Figure 1A). Using the above-mentioned viral particles, we transduced untouched naive primary human B cells that are pre-activated with CD40 ligand in the presence of IL-4 and IL-21. Frequencies of mCherry$^+$ cells were quantified by flow cytometry (Figure 1B). Consistent with a previous report,[21] primary human B cells were efficiently transduced with GaLV-pseudotyped retroviral particles (Figure 1C). Interestingly, transduction efficiency was significantly higher with RD114-pseudotyped retroviruses in comparison with other tested viruses (Figure 1C). We conclude that RD114-pseudotyped retrovirus transduces primary human B cells with higher efficiency than other tested retroviral vectors.

Optimized protocols for efficient transduction of primary human B cells with RD114-and GaLV-pseudotyped retroviral vectors
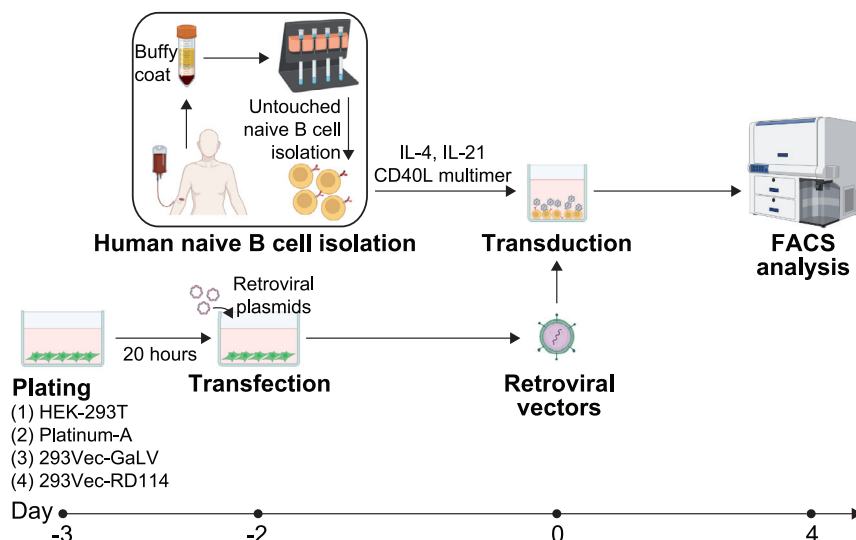Since primary human B cells can be efficiently transduced with RD114-or GaLV-pseudotyped retroviral particles, we next focused on establishing an optimal transduction protocol with these retroviral

systems. First, we examined whether an optimal virus titer could be obtained with different molecular ratios of main/packaging/envelope plasmids. We used the common ratio at 3:1:1 and increased 2-fold stepwise of the main plasmid, in total 1.5 μg DNA. The amount of each plasmid was calculated based on their sizes and ratios in the plasmid mixture (Table S1). Second, we tested whether distinct modes of B cell activation might contribute to transduction efficiency of primary human B cells. Here, we activated primary human B cells either with human CD40L multimer or mouse CD40L-expressing cell line (40LB cells) (Figure 2A). Regarding plasmid ratios, we found variations in transduction frequency with various plasmid ratios. Remarkably, ratios of 12:1:1, 24:1:1, and 48:1:1 gave the highest transduction efficiency in primary human B cells, and viral particles from the 293Vec-RD114 cell line gave a better transduction in comparison with viral particles from the other cell lines tested (Figure 2B). For the B cell activation conditions, we found a significantly elevated transduction frequency of primary human B cells activated with the CD40L multimer construct compared with CD40L expressing cell line (Figure 2C). We conclude that primary human B cells activated with CD40L multimers are more susceptible to RD114-pseudotyped retroviral transduction than those activated with the CD40L expressing cell line.

Highly efficient CRISPR-Cas9-mediated gene knockout of primary human B cells using RD114-pseudotyped retroviral vectors
To address whether RD114-pseudotyped retroviral vectors are able to deliver both sgRNA and Cas9 coding sequences to primary human B cells for gene knockout, we produced RD114-pseudotyped retroviral particles expressing either sgRNA or Cas9 to target the *β2M* (β2 microglobulin) gene. As for the sgRNA, we designed a sgRNA targeting the exon 1 of *β2M* gene and cloned it into the sgRNA plasmid carrying mCherry reporter (Figure 3A). It has been shown that the Furin recognition sequence allows a more efficient removal of T2A residues and that GSG linker enhances the ribosomal skip by T2A.[22–26] Therefore, and since we had to substitute mCherry by GFP in the MSCV-Cas9-T2A-mCherry plasmid, we included these sequences to increase the overall efficiency (Figure 3B). To deliver sgRNA and Cas9 components, we co-transduced human pre-activated B cells with sgRNA and Cas9 retroviral particles. Four days post transduction, sgRNA$^+$Cas9$^+$ (mCherry$^+$GFP$^+$) B cells were sorted and genomic DNA was extracted for analysis of insertion-deletion (Indel) frequencies. The remaining cells were examined for knockout efficacy at day 4 and day 8 through their β2M surface expression by flow cytometry (Figure 3C). Based on T7 endonuclease I (T7EI) assay and ICE analysis from purified co-transduced cells (Figure 3D), sgRNA targeting the *β2M* locus showed approximately 80% of gene knockout efficiency in primary human B cells (Figures 3E and 3F). FACS analysis at day 4 and 8 post transduction confirmed the gene editing efficiency with up to 80% of β2M$^-$ B cells (Figure 3G). Of note, only co-transduction with sgRNA and Cas9 give rise to editing, thus only in this condition we found a β2M$^-$ B cell population. Single transduction with only sgRNA or Cas9 did not show a β2M$^-$ B cell population (Figure S1).
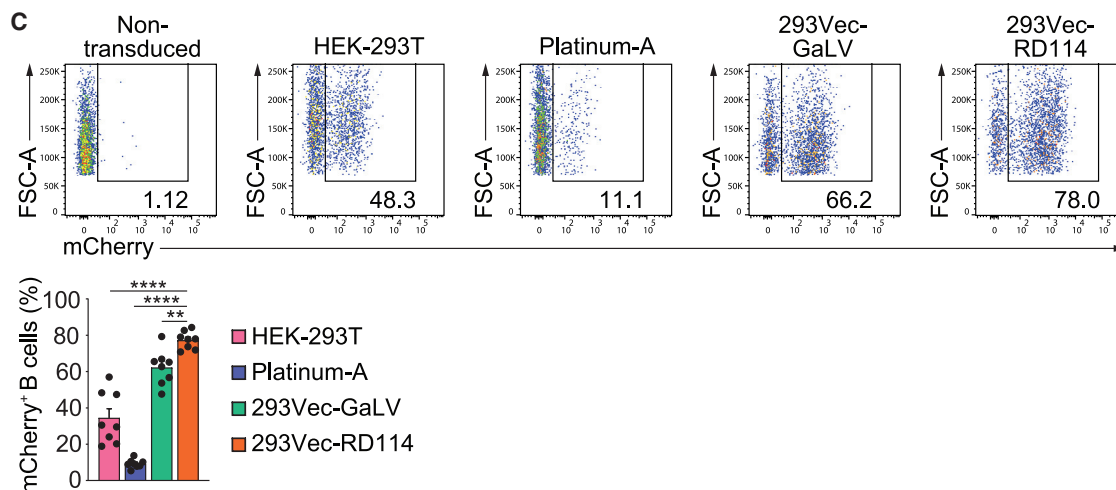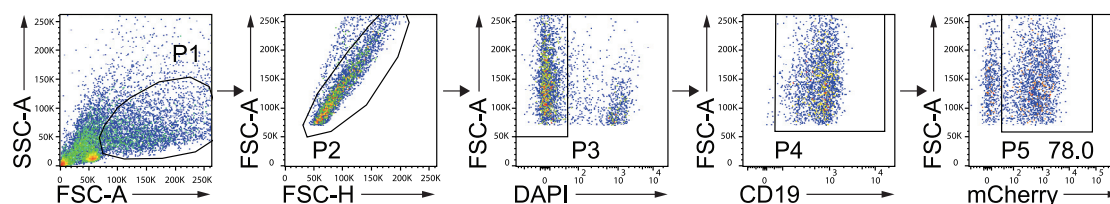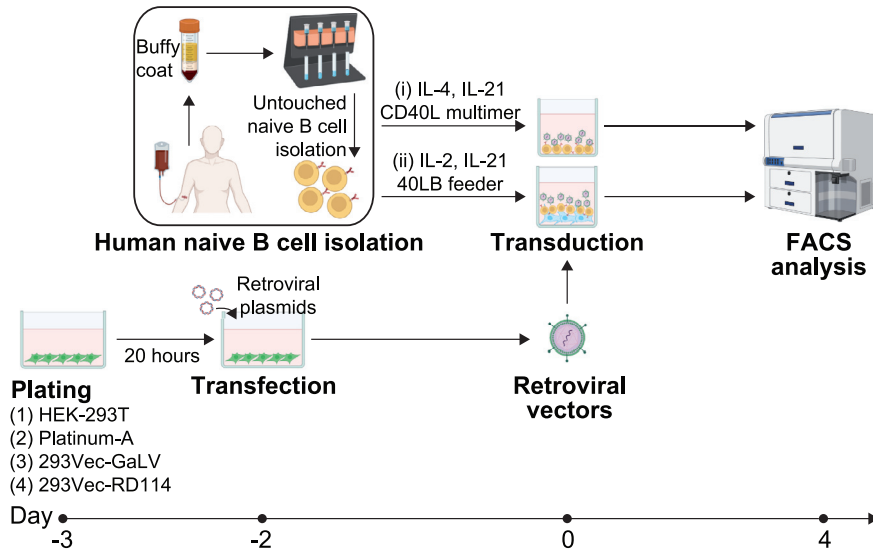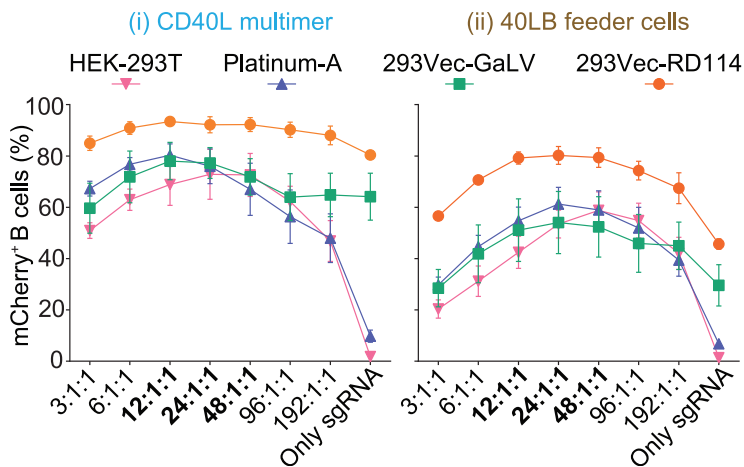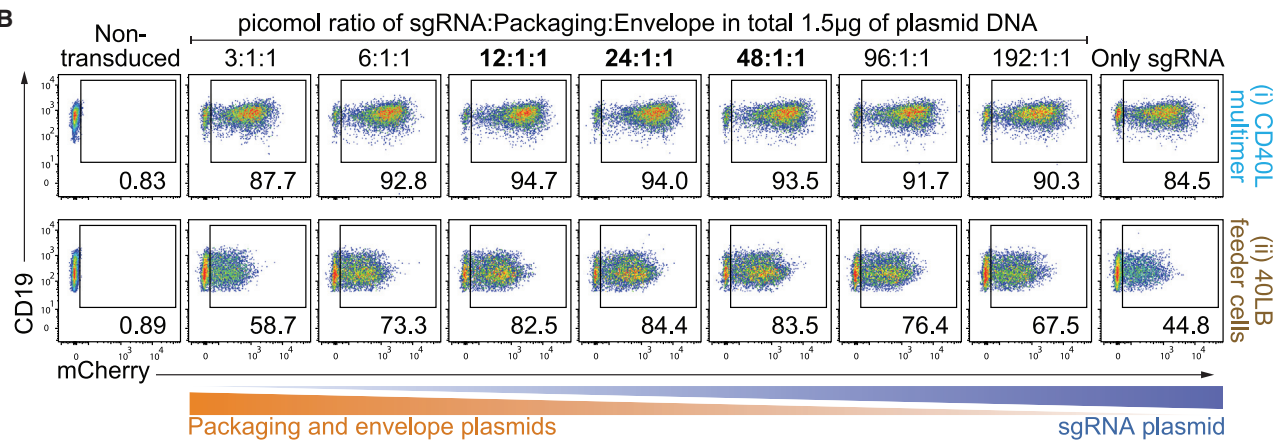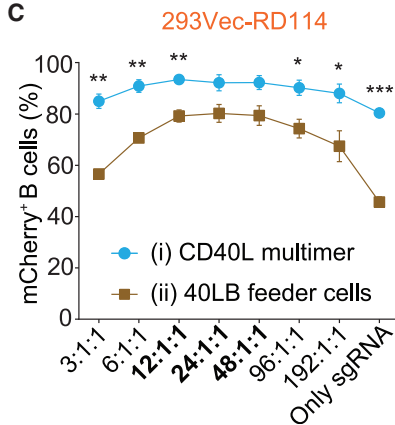
Figure 1. RD114-pseudotyped retroviral vectors efficiently transduce primary human B cells

(A) Experimental design. Human naive B cells were negatively selected from buffy coat and activated with human CD40L multimer in presence of IL-4 and IL-21 for 2 days. Simultaneously, retroviral packaging cell lines were plated for 20 h before transfection. Two days post transfection, retroviral supernatants were harvested and used for human B cell transduction. Transduced B cells were harvested on day 4 after transduction and analyzed by flow cytometry. (Created with BioRender.com). (B) Representative FACS plots show gating strategy to identify mCherry+ B cells at day 4 post transduction. (C) Representative FACS plots (top) and the graph (bottom) show the percentages of mCherry+ B cells 4 days post transduction. Non-transduced cells were used to define mCherry+ gate. HEK-293T was co-transfected with sgRNA plasmid, packaging plasmid (pHIT60), and envelope plasmid (GaLV WT); Platinum-A, 293Vec-GaLV, and 293Vec-RD114 were transfected with sgRNA plasmid only. Data were pooled from eight donors, shown as mean ± SEM. Statistical significance was calculated using one-way ANOVA test, only significant p values are shown: **$p < 0.01$; ****$p < 0.0001$.

A Workflow

B

(legend on next page)

CRISPR-Cas9-mediated *IRF4*, *PRDM1*, and *XBP1* knockout impairs plasma cell differentiation *in vitro*

IRF4, PRDM1, and XBP1 are known as the triad of PC master regulators in the mouse. Taking advantage of our CRISPR-Cas9 RD114-pseudotyped retroviral vectors, we targeted these loci and assessed the outcome on human B cell survival and PC differentiation. We designed sgRNAs to target *IRF4*, *PRDM1,* and *XBP1* at the exon 1, exon 7, and exon 2, respectively (Figure S2A). Then, we co-transduced human pre-activated B cells with Cas9 and sgRNA vectors. Four days after transduction, mCherry$^+$ GFP$^+$ B cells were sorted for T7EI assay and Indel analysis. As a result, gene-specific targeted human B cells showed at least 80% of gene editing efficiency at the targeted loci (Figures 4A, 4B, and S2B). To answer whether CRISPR-Cas9-mediated *IRF4*, *PRDM1,* and *XBP1* deficiencies lead to impaired survival and block of PC differentiation, we determined frequencies of mCherry$^+$GFP$^+$ B cells and CD27$^+$CD38$^+$ PCs at day 8 post transduction (day 4 post differentiation) using flow cytometry. Knocking out *IRF4* and *PRDM1* in primary human B cells resulted in a significant reduction of mCherry$^+$ GFP$^+$ B cells in comparison with non-targeted B cells, while *XBP1* gene knockout showed a slight reduction (Figure 4C). Consistent with data in the mouse,[13] we found a reduced frequency of CD27$^+$CD38$^+$ PCs among viable *IRF4-, PRDM1-,* and *XBP1*-deficient human B cells compared with non-targeted control cells (Figure 4D). Nonetheless, within the targeted cells, we were able to detect few CD27$^+$CD38$^+$ PCs, therefore further analysis addressed if these co-transduced CD27$^+$CD38$^+$ cells was edited. Thus, we sorted from *IRF4*-targeted and non-targeted samples mCherry$^+$ GFP$^+$, mCherry$^-$GFP$^-$, mCherry$^+$GFP$^+$CD27$^-$CD38$^-$, mCherry$^+$ GFP$^+$CD27$^-$CD38$^+$, and mCherry$^+$GFP$^+$CD27$^+$CD38$^+$ cells (Figure 4E). We analyzed those cell populations by T7EI assay and quantified Indel rate by Sanger sequencing combined with ICE analysis. Remarkably, the T7EIassay and Indel rate showed that the majority of differentiated PCs (mCherry$^+$GFP$^+$CD27$^+$CD38$^+$) and pre-plasmablasts (pre-PBs) (mCherry$^+$GFP$^+$CD27$^-$CD38$^+$) were not edited, while mCherry$^+$GFP$^+$CD27$^-$CD38$^-$ were edited properly for the target alleles (Figure 4E). Of note, total mCherry$^-$GFP$^-$ were wild type (Figure 4E). These results demonstrated that at the time of PC analysis (day 4 after differentiation) edited cells are absent from the PC population in contrast to co-transduced but not edited PCs. Intra-nuclear staining of IRF4, PRDM1, and XBP1 in sg*IRF4*, sg*PRDM1*, and *sgXBP1*-targeted samples confirmed the reduction of TF-expressing PC populations in total viable cells (Figure S2C). To further characterize that these TF-expressing PC cells were derived from non-targeted cells, we performed IRF4 intra-nuclear staining using mCherry$^+$GFP$^+$ and mCherry$^-$GFP$^-$ sorted from the same

IRF4-targeted samples at day 2 after differentiation (day 6 after transduction). Remarkably, we detected very few IRF4-expressing PCs in the sorted mCherry$^+$GFP$^+$ compared with mCherry$^-$GFP$^-$ (Figure 4F), demonstrating that the TF-expressing PC populations in total viable cells are mainly from non-targeted mCherry$^-$GFP$^-$ cells. We also found that *IRF4*-targeted cells failed to progress to pre-PB (CD27$^-$CD38$^+$) state, *PRDM1*-targeted cells failed to differentiate into PC (CD27$^+$CD38$^+$) state, while the survival of *XBP1*-targeted cells was substantially impaired (Figure 4D). Thus, we performed intra-nuclear staining of IRF4, PRDM1, and XBP1 in wild-type primary human B cells differentiated *in vitro* to examine at which state of the B cell differentiation process these TFs were expressed. We found that activated B cells (CD27$^-$CD38$^-$) and pre-PBs expressed similar levels of IRF4 while PBs/PCs expressed a notable increased level (Figure 4G). Additionally, PRDM1 started being expressed in pre-PBs and was increased in PB/PCs, while XBP1 was only expressed by PB/PCs (Figure 4G). These could explain that *IRF4*, *PRDM1,* and *XBP1*-targeted B cells failed to progress to the pre-PB, PC state and PC survival, respectively. We also found a down-regulated expression of PRDM1 in *IRF4*-targeted cells compared with non-targeted cells (Figure 4H) as reported by prior studies in mouse.[27,28] Collectively, we demonstrated that IRF4, PRDM1, and XBP1 are required for human B cell survival and PC differentiation.
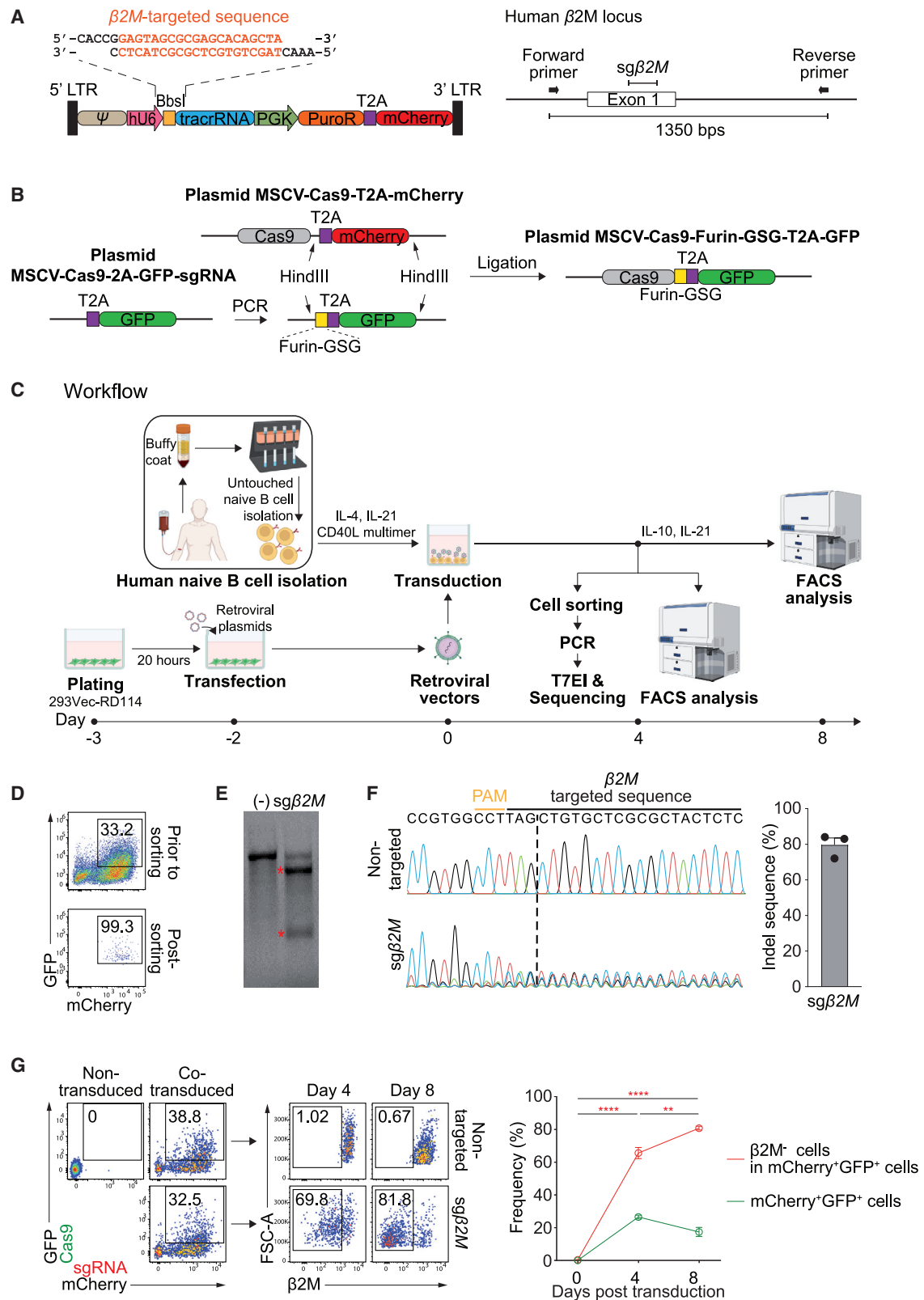
DISCUSSION

The delivery of CRISPR-Cas9 into cells is a crucial step in gene editing technology. In the mouse, to extend the utility of CRISPR-Cas9 technology, several Cas9 transgenic mice have been generated.[13,29–31] These mouse strains simplify and allow gene editing with high efficiency both *in vivo* and *ex vivo* as only sgRNAs are required for a successful gene knockout in Cas9-expressing cells. Previously, Cas9-expressing B cells transduced with sgRNA retroviral particles have been used to identify molecules involved in mouse B cell activation and PC differentiation.[13] However, the same systems are not available for human B cells. Thus, to apply such gene editing technology in human B cells, it is required to deliver both sgRNA and Cas9 components.

Generally, CRISPR-Cas9 can be delivered to human cells by three main approaches, namely (1) plasmid DNA expressing sgRNA and Cas9 protein delivered by viral vectors, (2) sgRNA and mRNA coding for Cas9 protein, and (3) ribonucleoprotein (RNP) containing sgRNA and Cas9 protein. Despite insertional mutagenesis and slow onset of editing, viral vectors are still the most appropriate delivery method for large-scale screening of human PC differentiation regulators *ex vivo*

Figure 2. Establishing efficient transduction conditions for primary human B cells with RD114-and GaLV-pseudotyped retroviral vectors

(A) Experimental design. Negatively selected human naive B cells were activated either with (i) human CD40L multimer in the presence of IL-4 and IL-21, or with (ii) 40LB feeder cells, in the presence of IL-2 and IL-21. 40LB feeder cells were irradiated (30 Gy) and plated 1 day prior to the B cell culture. (Created with BioRender.com). (B) Representative FACS plots (top) show the percentage of mCherry$^+$ B cells at day 4 post transduction using different plasmid conditions as indicated. Picomole of sgRNA plasmid increased as opposed of packaging and envelope plasmids, respectively. The graphs (bottom) show frequencies of mCherry + B cells obtained from three donors for condition (i) and (ii). (C) The graph shows the percentage of mCherry$^+$ B cells activated with condition (i) compared with condition (ii) at day 4 post transduction with retrovirus produced by the 293Vec-RD114 cell line. Groups were compared using unpaired t test, only significant p values are shown: *p < 0.1; **p < 0.01; ***p < 0.001. Data shown as mean ± SEM.

(legend on next page)

due to stable expression of sgRNA and Cas9, easy tracking of knockout cells, and cost advantages when compared with mRNA and RNP methods.[32] Unfavorably, Cas9 requires a large insert in plasmid DNA, which hinders the viral particle packaging process, resulting in low virus titers, and eventually impeding the delivery efficacy of Cas9 into target cells. Thus, a viral vector with superior transduction efficiency for primary human B cells would compensate for virus titer challenges.

Here, we documented a highly efficient delivery method of CRISPR-Cas9 that uses RD114-pseudotyped retroviral vectors to knockout candidate genes in primary human B cells and evaluate whether they abrogate PC differentiation. *IRF4, PRDM1,* and *XBP1*-targeted primary human B cells failed to differentiate into PCs, highlighting the crucial roles of these genes in human PC generation. Importantly, these findings show a shared involvement of IRF4, PRDM1, and XBP1 in PC differentiation between mouse and human.[10,13,33] Nevertheless, there are reports suggesting that XBP1 does not play a major role in controlling mouse PC differentiation.[34] In this study, we validated the use of ICE online program (https://ice.synthego.com/, Synthego) to quantify the Indel rate in the target samples by comparing the levels of β2M-knockout using flow cytometry and quantification Indel rate using ICE online program. The Indel rate was approximately 80% by ICE analysis (Figure 3F), in agreement with the phenotyping data by FACS analysis (Figure 3G). Collectively, our system has demonstrated feasibility for functional investigation of molecules expressed in human PCs, which may provide novel insights into biology and function of human PCs in health and disease.

While interesting, the system may have some limitations. For instance, due to a slow onset of gene editing by virus-based systems,[32] this approach may be inappropriate for identifying regulators of PCs differentiated from memory B cells, as these cells often rapidly differentiate into PC before the target gene is knocked out. Therefore, RD114-pseudotyped retroviral vectors should be tested on resting, non-activated or shortly activated B cells, to examine whether virus-mediated delivery of CRISPR-Cas9 can be used for identification of regulators of PC differentiation from memory B cells. Sequential transduction protocols for delivering of sgRNA and Cas9 could be more efficient; however, this would reduce the sensitivity to identify PC regulators, because (1) viral supernatant contains viral RNA, DNA, and proteins that can induce differentiation of B cells into PCs, and (2) sequential transduction protocols would require maintenance of B cells under activation conditions longer and this would induce the PC differentiation before the CRISPR-Cas9-meditated mutagenesis becomes effective. We considered that the all-in-one plasmid containing both Cas9 and sgRNA might be advantageous in terms of transduction and editing efficiency. However, with this approach we achieved a lower transduction and knockout efficacy compared with co-transduction (data not shown). We believe that the size of the all-in-one plasmid exceeds the retroviral particle packaging capacity, resulting in a very low virus titer.

In conclusion, our approach allows knockout of molecules up-regulated in activated B cells, plasmablasts, and PCs in order to gain better understanding of the molecular mechanisms governing B cell activation, and survival, PC differentiation, and antibody secretion.
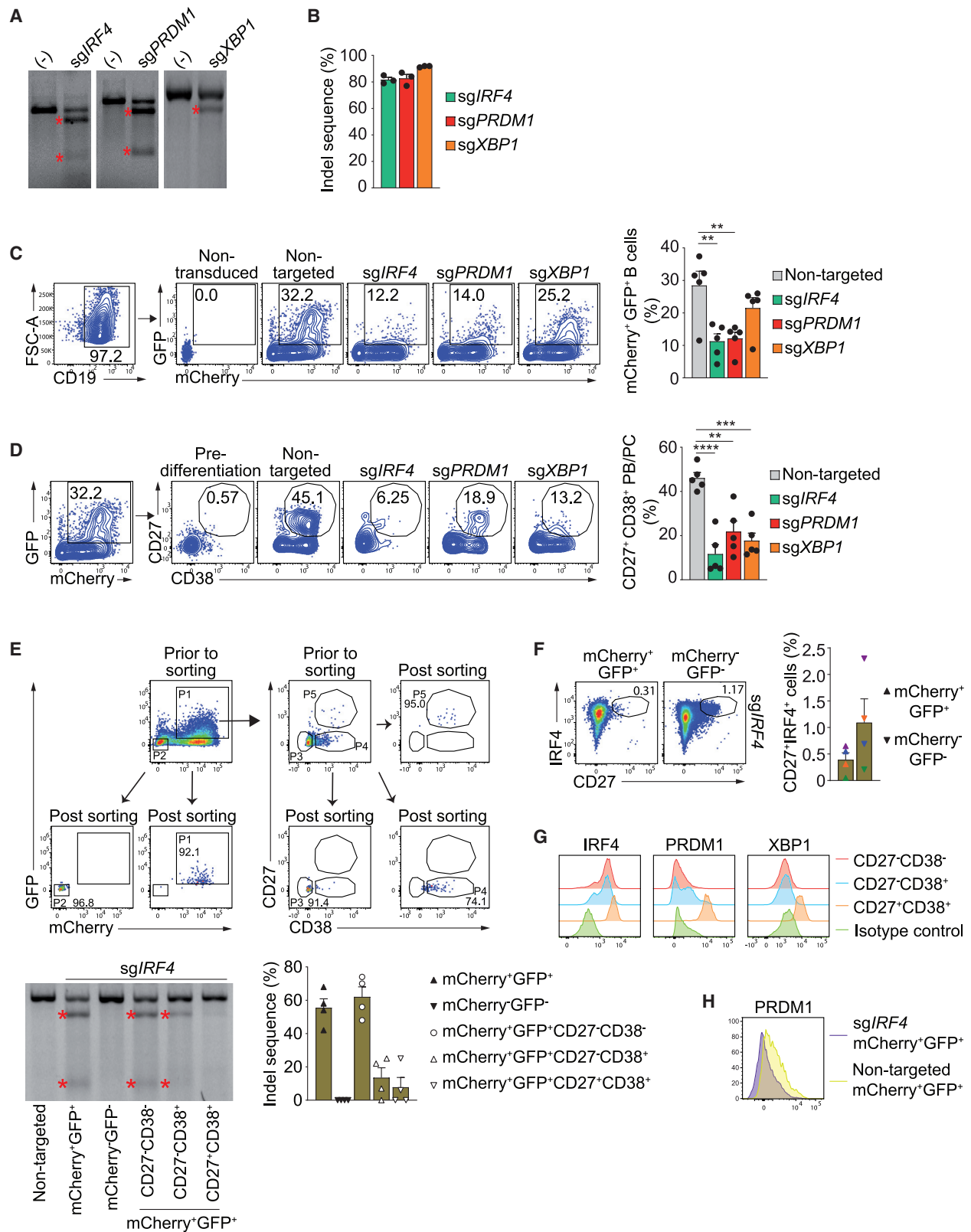
MATERIALS AND METHODS

Human buffy coats
Buffy coats of three female and 11 male healthy donors, age from 18 were provided by DRK-Blutspendedienst Nord-Ost (https://www.blutspende-nordost.de/). This study was reviewed and approved by the ethics committee of Charité Universitätsmedizin Berlin in accordance with Declaration of Helsinki.

Human naive B cell culture
Human PBMCs were isolated from buffy coats of healthy donors by Ficoll Density Gradient method and cryo-preserved at −80 °C. Human naive B cells were isolated from frozen PBMCs with Naive B cell isolation kit II (Miltenyi Biotec, Cat. #130-091-150). In brief, frozen PBMCs were washed with PBS/BSA/EDTA, then incubated with Biotin-Antibody Cocktail for 15 min. Cells were washed again with PBS/BSA/EDTA and incubated with Anti-Biotin MicroBeads

Figure 3. Efficient CRISPR-Cas9-mediated knockout of *β2M* housekeeping gene in primary human B cells

(A) *β2M*-specific targeting sequence was inserted into BbsI restriction site of sgRNA plasmid (left). The scheme shows the targeted site of *β2M* exon 1 and two primer sites for amplifying the flanking region of *β2M*-targeted site by PCR (right). (B) The sequence of T2A-GFP was amplified from plasmid MSCV-Cas9-2A-GFP-sgRNA and Furin-GSG sequence was included in the forward primer. HindIII restriction sites were added in both forward and reverse primers. The amplified fragment was digested with HindIII enzyme and replaced for T2A-mCherry sequence in plasmid MSCV-Cas9-T2A-mCherry. The reconstructed plasmid carries sequences of Cas9-Furin-GSG-T2A-GFP. (C) Experimental design. Negatively selected human naive B cells were activated with CD40L multimer in presence of IL-4 and IL-21 for 2 days. In parallel, 293Vec-RD114 retroviral packaging cells were plated for 20 h until transfection. Two days post transfection, retroviral supernatant was harvested for transduction. Day 4 post transduction, a half of B cells was harvested for FACS analysis or cell sorting and the other half was remained in culture with IL-10 and IL-21 for another 4 days. (Created with BioRender.com). (D) Representative FACS plots show co-transduced B cells before (top) and after (bottom) sorting at day 4 post transduction. (E) Agarose gel from T7 endonuclease I assay shows digested bands from sg*β2M*-targeted compared with non-targeted sample. sg*β2M*: sgRNA plasmid with *β2M*-targeted sequence; (−): non-targeted. Red asterisks highlight the digested DNA bands. (F) Sanger sequencing signal traces (left) show noise peaks at *β2M*-targeted site compared with non-targeted sample. The dashed line indicates cleavage site of Cas9. The graph (right) shows the percentage of Indel mutations at *β2M*-targeted site compared with non-targeted sample. Alignment and the percentage of Indel mutations were performed by ICE analysis online program (Synthego). (G) Representative FACS plots show co-transduced B cells with both sgRNA (mCherry) and Cas9 (GFP) (left) and β2M⁻ B cells (right) at day 4 and 8 post transduction. mCherry⁺GFP⁺ B cells were gated based on non-transduced sample, β2M⁻ B cells were gated based on non-targeted sample (transduced with sgRNA and Cas9 plasmids but sgRNA has no targeted sequence). The graph (right) shows the percentage of mCherry⁺GFP⁺ and surface β2M⁻ B cells in mCherry⁺GFP⁺ cells at day 0, 4, and 8 post transduction. Statistical significance was calculated using the unpaired t test: **p < 0.01; ****p < 0.0001. Data were pooled from three donors (F) and six donors (G), shown as mean ± SEM.

for 15 min. Finally, cells were washed and transferred onto magnetically applied LS column (Miltenyi Biotec, Cat. #130-042-401) for separation. Untouched naive B cells were collected from negative fraction with purity > 95% according to $CD19^+CD3^-$. Human naive B cells (5×10^4 cells/well in 96-well plate) were cultured in RPMI-1640 GlutaMAX medium (Gibco, Cat. #61870-010) supplied with 10% (v/v) FBS (Corning, Cat. #35-079-CV), 1 mM Sodium Pyruvate (Gibco, Cat. #11360-039), 100 U/mL Penicillin (Gibco, Cat. #15140-122), 100 μg/mL Streptomycin (Gibco, Cat. #15140-122), 50 μM 2-mercaptoethanol (Gibco, Cat. #31350-010), and 25 mM HEPES (Gibco, Cat. #15630056). Human naive B cells were activated either with (1) human CD40L multimer (1 μg/mL) (Miltenyi Biotec, Cat. #130-098-776) in presence of IL-4 (10 ng/mL) and IL-21 (10 ng/mL), or with (2) 30 Gy irradiated 40LB feeder cells (1.5×10^4 cells/well in 96-well plate) in presence of IL-2 (5 ng/mL) and IL-21 (10 ng/mL) for 2 days before retroviral transduction. Day 4 post transduction, the transduced B cells were further cultured in PC differentiation medium containing IL-10 (10 ng/mL) and IL-21 (10 ng/mL). B cells were analyzed by flow cytometry in different time points. All recombinant human cytokines were purchased from Peprotech.

Cell lines
Platinum-A cell line was a kind gift from Dr. Toshio Kitamura's laboratory (The University of Tokyo, Tokyo, Japan). 293Vec-GaLV and 293Vec-RD114 cell lines were kind gifts from BioVec Pharma (Canada), and 40LB cell line expressing mouse CD40 ligand was a kind gift from Dr. Daisuke Kitamura's laboratory (Tokyo University of Science, Tokyo, Japan). HEK-293T, Platinum-A, 293Vec-GaLV, 293Vec-RD114, and 40LB cell lines were cultured in DMEM GlutaMAX medium (Gibco, Cat. #61965-026) supplemented with 10% (v/v) FBS (Corning, Cat. #35-079-CV), 1 mM Sodium Pyruvate (Gibco, Cat. #11360-039), 100 U/mL Penicillin (Gibco, Cat. #15140-122), 100 μg/mL Streptomycin (Gibco, Cat. #15140-122), 50 μM 2-mercaptoethanol (Gibco, Cat. #31350-010), and 25 mM HEPES (Gibco, Cat. #15630056).

Plasmid constructs
Packaging (pHIT60) and envelope (GaLV WT) plasmids were kind gifts from Dr. Daniel James Hodson's laboratory (Wellcome-MRC Cambridge Stem Cell Institute, Cambridge, UK). MSCV-Cas9-Furin-GSG-T2A-GFP vector was modified from MSCV-Cas9-T2A-mCherry plasmid by replacing T2A-mCherry fragment with Furin-GSG-T2A-GFP fragment. T2A-GFP fragment was cloned from MSCV-Cas9-2A-GFP-sgRNA plasmid (Addgene, Cat. #124889, RRID: Addgene_124889) (Figure 3A). MSCV-hU6-sgRNA-PGK-PuroR-T2A-mCherry and MSCV-Cas9-Furin-GSG-T2A-GFP plasmids were termed as sgRNA and Cas9 plasmids hereafter, respectively. The sgRNAs targeting *β2M*, *IRF4*, *PRDM1*, and *XBP1* loci were designed using CrispRGold program,[13] and cloned into sgRNA plasmid as previously described.[35] The oligonucleotides and primer sequences are shown in Table S2. All plasmids were transformed into One Shot™ TOP10 Chemically Competent *E. coli* (Invitrogen, Cat. #C404003), the bacteria were then cultured in LB medium (MP Biomedical, Cat. #3002031) supplemented with 100 μg/mL Ampicillin (Sigma-Aldrich, Cat. #A5354-10ML) overnight, and the plasmids were purified using Nucleospin plasmid mini kit (Macherey-Nagel, Cat. #740588.250).

Retroviral production and transduction
HEK-293T, Platinum-A, 293Vec-GaLV, or 293Vec-RD114 cells were plated 20 h in complete DMEM medium before transfection (5×10^5 cells/well in 6-well plate). A plasmid DNA mixture (total 1.5 μg) containing sgRNA or Cas9, packaging, and envelope plasmids was diluted in Opti-MEM medium (Gibco, Cat. #31985-047), mixed with P3000 reagent, then Lipofectamine 3000 reagent (Invitrogen, Cat. #L3000015) and incubated at room temperature for 15 min

---

Figure 4. *IRF4*, *PRDM1*, and *XBP1* are crucial for B cell survival and PC differentiation *in vitro*

(A) Agarose gel from T7 endonuclease I assay shows digested bands from sg*IRF4*, sg*PRDM1*, and sg*XBP1*-targeted compared to non-targeted samples, (−): non-targeted; sg*IRF4*, sg*PRDM1*, sg*XBP1*: sgRNA plasmid with targeted sequence of each gene, respectively. Red asterisks mark the corresponding digested DNA bands. (B) The graph shows the percentage of Indel mutations at *IRF4*, *PRDM1*, and *XBP1*-specific targeted site compared with non-targeted samples. Alignment and the percentage of Indel mutations were performed by ICE analysis online program (Synthego). (C) Representative FACS plots (left) and graph (right) show the percentage of co-transduced B cells gated on $CD19^+$ B cells from non-transduced, non-targeted, sg*IRF4*, sg*PRDM1*, and sg*XBP1*-targeted samples. (D) Representative FACS plots (left) and graph (right) show the percentage of the PC population gated on co-transduced B cells from pre-differentiation and post differentiation, non-targeted, sg*IRF4*, sg*PRDM1*, and sg*XBP1*-targeted samples. (E) FACS plots (top) show gating strategy to identify populations for cell sorting and cell purity post sorting at day 6 post transduction (day 2 post differentiation). P1-5 are $mCherry^+GFP^+$, $mCherry^-GFP^-$, $mCherry^+GFP^+CD27^-CD38^-$, $mCherry^+GFP^+CD27^-CD38^+$ and $mCherry^+GFP^+CD27^+CD38^+$, respectively. Agarose gel from T7 endonuclease I assay (left bottom) shows digested bands for $mCherry^+GFP^+$, $mCherry^-GFP^-$, $mCherry^+GFP^+CD27^-CD38^-$, $mCherry^+GFP^+CD27^-CD38^+$, and $mCherry^+GFP^+CD27^+CD38^+$ sorted from *IRF4*-targeted cells compared with non-targeted cells. Red asterisks mark the corresponding digested DNA bands. The graph (right bottom) shows the percentage of Indel mutations at *IRF4*-targeted site compared with non-targeted sample of indicated cell populations. Alignment and the percentage of Indel mutations were performed by ICE analysis online program (Synthego). (F) Representative FACS plots (left) and the graph (right) show the percentage of $IRF4^+CD27^+$ cells in $mCherry^+GFP^+$ and $mCherry^-GFP^-$ cells sorted from the same *IRF4*-targeted samples. The color coding indicates samples from the same donor. (G) Representative histograms show the expression of IRF4, PRDM1 and XBP1 in $CD27^-CD38^-$, $CD27^-CD38^+$, and $CD27^+CD38^+$ WT cells. (H) Representative histogram shows expression of PRDM1 in sorted $mCherry^+GFP^+$ cells from *IRF4*-targeted compared with non-targeted samples. Cells were analyzed or used for cell sorting at day 4 post transduction (prior differentiation) (A and B), day 8 post transduction (day 4 post differentiation) (C and D), and day 6 post transduction (day 2 post differentiation) (E–H). Data were representative or pooled from three donors (A and B), five donors (C and D), and four donors (E–H), shown as mean ± SEM. Statistical significance was calculated using one-way ANOVA test (C and D), only significant p values are shown: **$p < 0.01$; ***$p < 0.001$; ****$p < 0.0001$. Each gene was independently targeted by three different sgRNAs. Data for one sgRNA are shown.

before adding to the cell lines. Six hours later, Lipofectamine-contained medium was replaced with fresh medium for retroviral production.

Two days post transfection, retroviral supernatant was harvested and centrifuged at speed 500 × g for 10 min at room temperature to remove cell debris. Polybrene (Sigma-Aldrich, Cat. #TR-1003-G) (final concentration 10 μg/mL) was added to retroviral supernatant prior to transduction. Medium in each well of 2-day-activated B cells was replaced with 200 μL of viral supernatant, followed by a 1,500 × g centrifugation for 3 h at 32°C. Volume of sgRNA and Cas9 retroviral supernatant was mixed 100μL:100μL for co-transduction. Immediately after centrifugation, retroviral supernatant was replaced with complete RPMI medium (Gibco, Cat. #61870-010) supplied with (1) human CD40L multimer (1 μg/mL), IL-4 (10 ng/mL), and IL-21 (10 ng/mL) or (2) IL-2 (5 ng/mL) and IL-21 (10 ng/mL). The B cells were maintained for 4 more days until cell sorting, FACS analysis, or PC differentiation.

FACS analysis and cell sorting
For surface staining, cells before and after MACS isolation, at day 4 and day 8 post transduction were stained with antibodies against surface markers for 15 min. IRF4, PRDM1, and XBP1 intra-nuclear staining was performed with Foxp3 staining kit (Invitrogen, Cat. #00-5523-00). Dead cells were excluded by DAPI or LIVE/Dead Fixable Aqua Dead Cell Stain Kit (Invitrogen, Cat. #L34966). Stained cells were analyzed by BD LSRFortessa and BD FACSymphony A5.

For cell sorting, B cells were harvested at day 4 and day 6 post transduction (day 2 after differentiation), stained with DAPI, CD27, and CD38, and sorted for DAPI⁻mCherry⁺GFP⁺ cells (day 4 post transduction) and DAPI⁻mCherry⁺GFP⁺, DAPI⁻mCherry⁻GFP⁻, DAPI⁻mCherry⁺GFP⁺CD27⁻CD38⁻, DAPI⁻mCherry⁺GFP⁺CD27⁻CD38⁺, DAPI⁻mCherry⁺GFP⁺CD27⁺CD38⁺ cells (day 6 post transduction) on BD FACSAria II Cell Sorter.

Antibodies
All antibodies used in this study are anti-human specific monoclonal antibodies. CD3-Pacific Orange (Clone OKT3) and CD19-Alexa488 (Clone BU12) were produced in-house at DRFZ. CD19-PE/Cy7 (Clone HIB19, eBioscience, Cat. #25-0199-42, RRID: AB_1582278), CD27-BV786 (Clone L128, BD Biosciences, Cat. #563327, RRID: AB_2744353), CD38-APC/Cy7 (Clone HIT2, Biolegend, Cat. #303534, RRID: AB_2561605), IRF4-PerCP/Cy5.5 (Clone IRF4.3E4, Biolegend, Cat. #646415, RRID: AB_2728481), BLIMP1/PRDM1-APC (Clone 646702, R&D Systems, Cat. #IC36081A, RRID: AB_11128645), XBP-1S-BV421 (Clone Q3-695, BD Biosciences, Cat. #563382, RRID: AB_2738168), β2M-APC (Clone 2M2, Biolegend, Cat. #316312, RRID: AB_10641281), Mouse IgG1 κ Isotype Control-APC (Clone MOPC-21, Biolegend, Cat. #400121, RRID: AB_326443), Mouse IgG1, κ Isotype Control-BV421 (Clone X40, BD Biosciences, Cat. #562438, RRID: AB_11207319), Rat IgG1, κ Isotype Control-PerCP/Cy5.5 (Clone RTK2071, Biolegend, Cat. #400425, RRID: AB_893689).

Genomic DNA extraction
Sorted B cells were mixed with QuickExtract DNA extraction solution (Lucigen, Cat. #QE09050), following with a thermal cycle consist of 65–68–95°C, 15 min each step and pause at 4°C. Genomic DNA solution was stored at −20°C as template for PCR reactions amplifying DNA sequence at CRISPR-Cas9 targeted regions.

PCR, gel purification, and DNA sequencing
KOD polymerase (Sigma-Aldrich, Cat. #71086-3) was used for all PCR reactions; 2X KOD buffer was premixed as follows: 80 μL H_2O, 1,600 μL 5M Betaine (Sigma-Aldrich, Cat. #B0300-1VL), 400 μL DMSO (Sigma-Aldrich, Cat. #D2438), 800 μL 10X KOD buffer, 800 μL 2 mM dNTPs, and 320 μL 25 mM $MgSO_4$. Each 20 μL of PCR master mix consisted of 7.6 μL H_2O, 10 μL 2X KOD buffer, 0.5 μL 10 μM each primer, 0.4 μL KOD polymerase, and 1 μL DNA template. The PCR cycler was set as follow: 95°C for 5 min, 40 cycles of (95°C 20s, 58–62°C 20s, 70 °C 30 s/1 kb), 70 °C for 5 min, and 4 °C pause. The PCR products were separated on 1% agarose gel. The corresponding DNA bands were excised and purified using NucleoSpin Gel and PCR clean-up kit (Macherey-Nagel, Cat. #740.609.250), and dispatched to Eurofins Genomics for sequencing.

T7 endonuclease I assay
Flanking regions of CRISPR-Cas9 targeted sites were amplified by PCR and purified as described above. The purified PCR products were re-annealed as follows: 95°C for 5 min, ramp down to 85°C at 2°C/s rate, ramp down to 25°C at 0.1°C/s rate, and pause at 4°C. The re-annealed PCR products were incubated with T7 Endonuclease I (NEB, Cat. #M0302L) at 37°C for 15 min, the reaction was stopped by adding 0.25M EDTA. The digested PCR products were analyzed on 1% agarose gel for visualization.

Insertion-deletion analysis
The sequencing results of purified PCR products at CRISPR-Cas9 targeted regions were analyzed with Inference of CRISPR Edits (ICE) analysis online program (https://ice.synthego.com/, Synthego). In brief, the sequencing signal traces of CRISPR-Cas9 targeted sample was compared with non-targeted sample. On that basis, the ICE algorithm identifies the percentage of modified sequence with insertion or deletion mutations (Indel mutations).

Data analysis and statistics
Flow cytometry data were analyzed with FlowJo software (v10.8.1, https://flowjo.com/). Data quantification and statistical significance was performed using GraphPad Prism 9 (https://graphpad.com). Groups were compared using one-way ANOVA test or unpaired or paired t test; considered p values were indicated for each figure: *$p < 0.1$; **$p < 0.01$; ***$p < 0.001$; ****$p < 0.0001$.

DATA AVAILABILITY STATEMENT
This study did not generate/analyze any datasets/code. All other data will be made available upon written request to the corresponding author.

SUPPLEMENTAL INFORMATION

Supplemental information can be found online at https://doi.org/10.1016/j.omtn.2022.11.016.

AUTHOR CONTRIBUTIONS

T.A.L., V.T.C., A.C.L., K.R., T.D., and V.D.D. developed the study concept. T.A.L., V.T.C., A.C.L., E.S., C.K., D.H., K.R., T.D., and V.D.D. performed experiments and contributed to project development, data discussions, and preparation of the manuscript. All authors read and approved the submitted version of the article.

DECLARATION OF INTERESTS

The authors declare no competing interests.

REFERENCES

1. Lino, A.C., Dang, V.D., Lampropoulou, V., Welle, A., Joedicke, J., Pohar, J., Simon, Q., Thalmensi, J., Baures, A., Flühler, V., et al. (2018). LAG-3 inhibitory receptor expression identifies immunosuppressive natural regulatory plasma cells. Immunity 49, 120–133.e9.

2. Shen, P., Roch, T., Lampropoulou, V., O'Connor, R.A., Stervbo, U., Hilgenberg, E., Ries, S., Dang, V.D., Jaimes, Y., Daridon, C., et al. (2014). IL-35-producing B cells are critical regulators of immunity during autoimmune and infectious diseases. Nature 507, 366–370.

3. Dang, V.D., Stefanski, A.L., Lino, A.C., and Dörner, T. (2022). B- and plasma cell subsets in autoimmune diseases: translational perspectives. J. Invest. Dermatol. 142, 811–822.

4. Dang, V.D., Hilgenberg, E., Ries, S., Shen, P., and Fillatreau, S. (2014). From the regulatory functions of B cells to the identification of cytokine-producing plasma cell subsets. Curr. Opin. Immunol. 28, 77–83.

5. Dang, V.D., Mohr, E., Szelinski, F., Le, T.A., Ritter, J., Hinnenthal, T., Stefanski, A.L., Schrezenmeier, E., Ocvirk, S., Hipfl, C., et al. (2022). CD39 and CD326 are bona fide markers of murine and human plasma cells and identify a bone marrow specific plasma cell subpopulation in lupus. Front. Immunol. 13, 873217.

6. Wiedemann, A., Lettau, M., Wirries, I., Jungmann, A., Salhab, A., Gasparoni, G., Mei, H.E., Perka, C., Walter, J., Radbruch, A., et al. (2020). Human IgA-expressing bone marrow plasma cells characteristically upregulate programmed cell death protein-1 upon B cell receptor stimulation. Front. Immunol. 11, 628923.

7. Lee, J.U., Kim, L.K., and Choi, J.M. (2018). Revisiting the concept of targeting NFAT to control T cell immunity and autoimmune diseases. Front. Immunol. 9, 2747.

8. Huang, J., Wang, S., Jia, Y., Zhang, Y., Dai, X., and Li, B. (2020). Targeting FOXP3 complex ensemble in drug discovery. Adv. Protein Chem. Struct. Biol. 121, 143–168.

9. Bushweller, J.H. (2019). Targeting transcription factors in cancer - from undruggable to reality. Nat. Rev. Cancer 19, 611–624.

10. Nutt, S.L., Hodgkin, P.D., Tarlinton, D.M., and Corcoran, L.M. (2015). The generation of antibody-secreting plasma cells. Nat. Rev. Immunol. 15, 160–171.

11. Tellier, J., and Nutt, S.L. (2017). Standing out from the crowd: how to identify plasma cells. Eur. J. Immunol. 47, 1276–1279.

12. Tellier, J., Shi, W., Minnich, M., Liao, Y., Crawford, S., Smyth, G.K., Kallies, A., Busslinger, M., and Nutt, S.L. (2016). Blimp-1 controls plasma cell function through the regulation of immunoglobulin secretion and the unfolded protein response. Nat. Immunol. 17, 323–330.

13. Chu, V.T., Graf, R., Wirtz, T., Weber, T., Favret, J., Li, X., Petsch, K., Tran, N.T., Sieweke, M.H., Berek, C., et al. (2016). Efficient CRISPR-mediated mutagenesis in primary immune cells using CrispRGold and a C57BL/6 Cas9 transgenic mouse line. Proc. Natl. Acad. Sci. USA 113, 12514–12519.

14. Voss, J.E., Gonzalez-Martin, A., Andrabi, R., Fuller, R.P., Murrell, B., McCoy, L.E., Porter, K., Huang, D., Li, W., Sok, D., et al. (2019). Reprogramming the antigen specificity of B cells using genome-editing technologies. Elife 8, e42995.

15. Akidil, E., Albanese, M., Buschle, A., Ruhle, A., Pich, D., Keppler, O.T., and Hammerschmidt, W. (2021). Highly efficient CRISPR-Cas9-mediated gene knockout in primary human B cells for functional genetic studies of Epstein-Barr virus infection. PLoS Pathog. 17, e1009117.

16. Johnson, M.J., Laoharawee, K., Lahr, W.S., Webber, B.R., and Moriarity, B.S. (2018). Engineering of primary human B cells with CRISPR-Cas9 targeted nuclease. Sci. Rep. 8, 12144.

17. Wu, C.A.M., Roth, T.L., Baglaenko, Y., Ferri, D.M., Brauer, P., Zuniga-Pflucker, J.C., Rosbe, K.W., Wither, J.E., Marson, A., and Allen, C.D.C. (2018). Genetic engineering in primary human B cells with CRISPR-Cas9 ribonucleoproteins. J. Immunol. Methods 457, 33–40.

18. Caeser, R., Di Re, M., Krupka, J.A., Gao, J., Lara-Chica, M., Dias, J.M.L., Cooke, S.L., Fenner, R., Usheva, Z., Runge, H.F.P., et al. (2019). Genetic modification of primary human B cells to model high-grade lymphoma. Nat. Commun. 10, 4543.

19. Caeser, R., Gao, J., Di Re, M., Gong, C., and Hodson, D.J. (2021). Genetic manipulation and immortalized culture of ex vivo primary human germinal center B cells. Nat. Protoc. 16, 2499–2519.

20. Ghani, K., Wang, X., de Campos-Lima, P.O., Olszewska, M., Kamen, A., Rivière, I., and Caruso, M. (2009). Efficient human hematopoietic cell transduction using RD114- and GALV-pseudotyped retroviral vectors produced in suspension and serum-free media. Hum. Gene Ther. 20, 966–974.

21. Mock, U., Thiele, R., Uhde, A., Fehse, B., and Horn, S. (2012). Efficient lentiviral transduction and transgene expression in primary human B cells. Hum. Gene Ther. Methods 23, 408–415.

22. Chng, J., Wang, T., Nian, R., Lau, A., Hoi, K.M., Ho, S.C.L., Gagnon, P., Bi, X., and Yang, Y. (2015). Cleavage efficient 2A peptides for high level monoclonal antibody expression in CHO cells. MAbs 7, 403–412.

23. Fang, J., Qian, J.J., Yi, S., Harding, T.C., Tu, G.H., VanRoey, M., and Jooss, K. (2005). Stable antibody expression at therapeutic levels using the 2A peptide. Nat. Biotechnol. 23, 584–590.

24. Fang, J., Yi, S., Simmons, A., Tu, G.H., Nguyen, M., Harding, T.C., VanRoey, M., and Jooss, K. (2007). An antibody delivery system for regulated expression of therapeutic levels of monoclonal antibodies in vivo. Mol. Ther. 15, 1153–1159.

25. Lin, J., Neo, S.H., Ho, S.C.L., Yeo, J.H.M., Wang, T., Zhang, W., Bi, X., Chao, S.H., and Yang, Y. (2017). Impact of signal peptides on furin-2A mediated monoclonal antibody secretion in CHO cells. Biotechnol. J. 12, 1700268.

26. Liu, Z., Chen, O., Wall, J.B.J., Zheng, M., Zhou, Y., Wang, L., Vaseghi, H.R., Qian, L., and Liu, J. (2017). Systematic comparison of 2A peptides for cloning multi-genes in a polycistronic vector. Sci. Rep. 7, 2193.

27. Ochiai, K., Maienschein-Cline, M., Simonetti, G., Chen, J., Rosenthal, R., Brink, R., Chong, A.S., Klein, U., Dinner, A.R., Singh, H., and Sciammas, R. (2013). Transcriptional regulation of germinal center B and plasma cell fates by dynamical control of IRF4. Immunity 38, 918–929.

28. Sciammas, R., Shaffer, A.L., Schatz, J.H., Zhao, H., Staudt, L.M., and Singh, H. (2006). Graded expression of interferon regulatory factor-4 coordinates isotype switching with plasma cell differentiation. Immunity 25, 225–236.

29. Platt, R.J., Chen, S., Zhou, Y., Yim, M.J., Swiech, L., Kempton, H.R., Dahlman, J.E., Parnas, O., Eisenhaure, T.M., Jovanovic, M., et al. (2014). CRISPR-Cas9 knockin mice for genome editing and cancer modeling. Cell 159, 440–455.

30. Chu, V.T., Weber, T., Graf, R., Sommermann, T., Petsch, K., Sack, U., Volchkov, P., Rajewsky, K., and Kühn, R. (2016). Efficient generation of Rosa26 knock-in mice using CRISPR-Cas9 in C57BL/6 zygotes. BMC Biotechnol. *16*, 4.

31. Dow, L.E., Fisher, J., O'Rourke, K.P., Muley, A., Kastenhuber, E.R., Livshits, G., Tschaharganeh, D.F., Socci, N.D., and Lowe, S.W. (2015). Inducible in vivo genome editing with CRISPR-Cas9. Nat. Biotechnol. *33*, 390–394.

32. Yip, B.H. (2020). Recent advances in CRISPR-Cas9 delivery strategies. Biomolecules *10*, E839.

33. Reimold, A.M., Iwakoshi, N.N., Manis, J., Vallabhajosyula, P., Szomolanyi-Tsuda, E., Gravallese, E.M., Friend, D., Grusby, M.J., Alt, F., and Glimcher, L.H. (2001). Plasma cell differentiation requires the transcription factor XBP-1. Nature *412*, 300–307.

34. Taubenheim, N., Tarlinton, D.M., Crawford, S., Corcoran, L.M., Hodgkin, P.D., and Nutt, S.L. (2012). High rate of antibody secretion is not integral to plasma cell differentiation as revealed by XBP-1 deficiency. J. Immunol. *189*, 3328–3338.

35. Chu, V.T., Graf, R., and Rajewsky, K. (2017). CRISPR-Cas9-Mediated in vitro mutagenesis in GC-like B cells. Methods Mol. Biol. *1623*, 135–145.

Supplemental information

Efficient CRISPR-Cas9-mediated

mutagenesis in primary human B cells

for identifying plasma cell regulators

Tuan Anh Le, Van Trung Chu, Andreia C. Lino, Eva Schrezenmeier, Christopher Kressler, Dania Hamo, Klaus Rajewsky, Thomas Dörner, and Van Duc Dang

Table S1: Amount of each plasmid in plasmid mixtures

Ratio (Main/Gag-Pol/Envelope)	Mol (picomole) [1]			DNA mass (µg) [2]			
	Main	Gag-Pol	Envelope	Main	Gag-Pol	Envelope	Total
3:1:1	0.16742	0.05581	0.05581	0.76	0.42	0.32	1.50
6:1:1	0.22262	0.03710	0.03710	1.00	0.28	0.22	1.50
12:1:1	0.26657	0.02221	0.02221	1.20	0.17	0.13	1.50
24:1:1	0.29577	0.01232	0.01232	1.33	0.10	0.07	1.50
48:1:1	0.31291	0.00652	0.00652	1.41	0.05	0.04	1.50
96:1:1	0.32224	0.00336	0.00336	1.45	0.03	0.02	1.50
192:1:1	0.32712	0.00170	0.00170	1.477	0.013	0.010	1.50
Only sgRNA (Main plasmid)	0.33215	0	0	1.50	0	0	1.50

Plasmid sizes (base pairs): Main (7,308), Gag-Pol (12,227), Envelope (9,345)

[1] Picomole calculation of each plasmid in total of 1.5 µg DNA:

$$P \text{ (picomole of } M_xG_yE_z) = \frac{1.5 \text{ (µg)} * 10e6}{(x*a + y*b + z*c)*617.96 + 36.04}$$

Picomole of Main plasmid = P*x
Picomole of Gag-Pol plasmid = P*y
Picomole of Envelope plasmid = P*z

$M_xG_yE_z$: Formula of plasmid mixture
M: Main plasmid
G: Gag-Pol plasmid
E: Envelope plasmid
x, y, z: Plasmid ratios (Main/Gag-Pol/Envelope)
a, b, c: Plasmid sizes (Main/Gag-Pol/Envelope) (base pairs)

[2] DNA mass calculation of each plasmid:

$$\text{DNA mass (µg)} = \frac{\text{Picomole of plasmid} * (\text{Plasmid size} * 617.96 + 36.04)}{10e6}$$

The calculations in Table S1 were adapted following formula at:
https://nebiocalculator.neb.com/#!/dsdnaamt

Table S2: Oligonucleotide and primer sequences

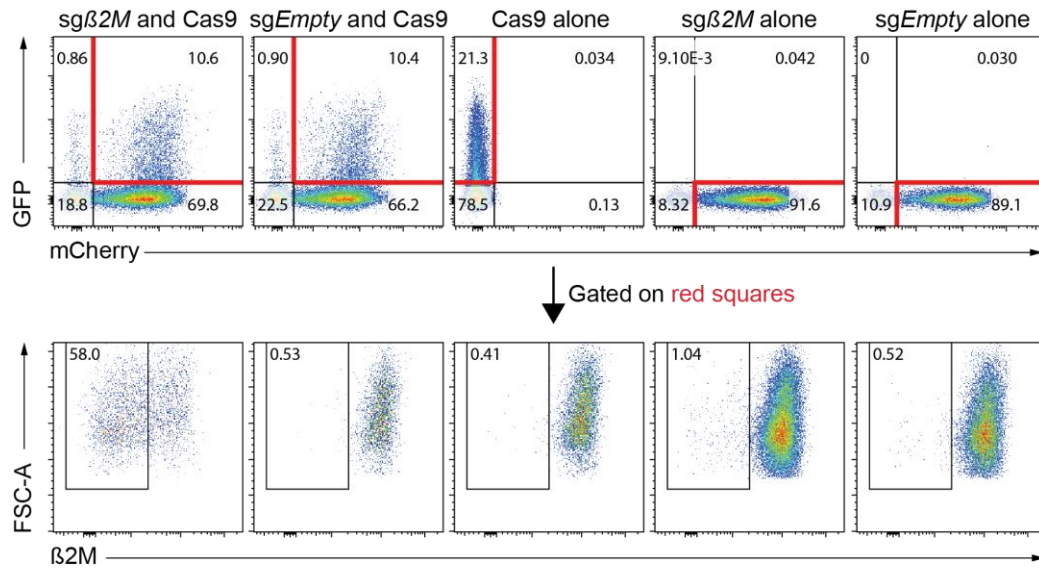| Name	Sequence (5'-3')	Purpose
hU6-forward	acgatacaaggctgttagagag	For sequencing of inserted gene specific targeting sequence
Furin-T2A-GFP-forward	aatgaaaagcttaggcggaagcgggggtcagg agagggcagaggaagtcttctaacatgcgg	Amplify T2A-GFP sequence from plasmid pMSCV-Cas9-2A-GFP-sgRNA (Addgene)
Furin-T2A-GFP-reverse	taacaaaagcttttacttgtacagctcgtccatgcc gaga	Amplify T2A-GFP sequence from plasmid pMSCV-Cas9-2A-GFP-sgRNA (Addgene)
sg*ß2M*-forward	caccggagtagcgcgagcacagcta	Human *ß2M* targeting sequence
sg*ß2M*-reverse	aaactagctgtgctcgcgctactcc	Human *ß2M* targeting sequence
ß2M-forward	gtcctagaatgagcgcccg	Amplify human *ß2M* locus
ß2M-reverse	tgctctggagaatctcacgc	Amplify human *ß2M* locus
sg*IRF4*-forward	caccgcaagcaggactacaaccgcg	Human *IRF4* targeting sequence
sg*IRF4*-reverse	aaaccgcggttgtagtcctgcttgc	Human *IRF4* targeting sequence
IRF4-forward	actgacagagtcgcggggaag	Amplify human *IRF4* locus
IRF4-reverse	agagccgaggcctcctttcctc	Amplify human *IRF4* locus
sg*PRDM1*-forward	caccgggatggggtaaacgacccga	Human *PRDM1* targeting sequence
sg*PRDM1*-reverse	aaactcgggtcgtttaccccatccc	Human *PRDM1* targeting sequence
PRDM1-forward	tcagttctctctagccctctgtgtaatcgc	Amplify human *PRDM1* locus
PRDM1-reverse	gactgctctctctcaaggcctaccttcag	Amplify human *PRDM1* locus
sg*XBP1*-forward	caccggactgccagagatcgaaaga	Human *XBP1* targeting sequence
sg*XBP1*-reverse	aaactctttcgatctctggcagtcc	Human *XBP1* targeting sequence
XBP1-forward	aattggactgggggacggag	Amplify human *XBP1* locus
XBP1-reverse	ataggggctgaaacaacttggg	Amplify human *XBP1* locus

Figure S1: Efficient CRISPR/Cas9-mediated knockout of *ß2M* housekeeping gene in primary human B cells. Representative FACS plots show the frequency of β2M⁻ B cells in sg*β2M*⁺Cas9⁺, sg*Empty*⁺Cas9⁺, Cas9⁺, sg*β2M*⁺ and sg*Empty*⁺ transduced B cells at day 4 after transduction. sg*Empty* is sgRNA without the targeted sequence.
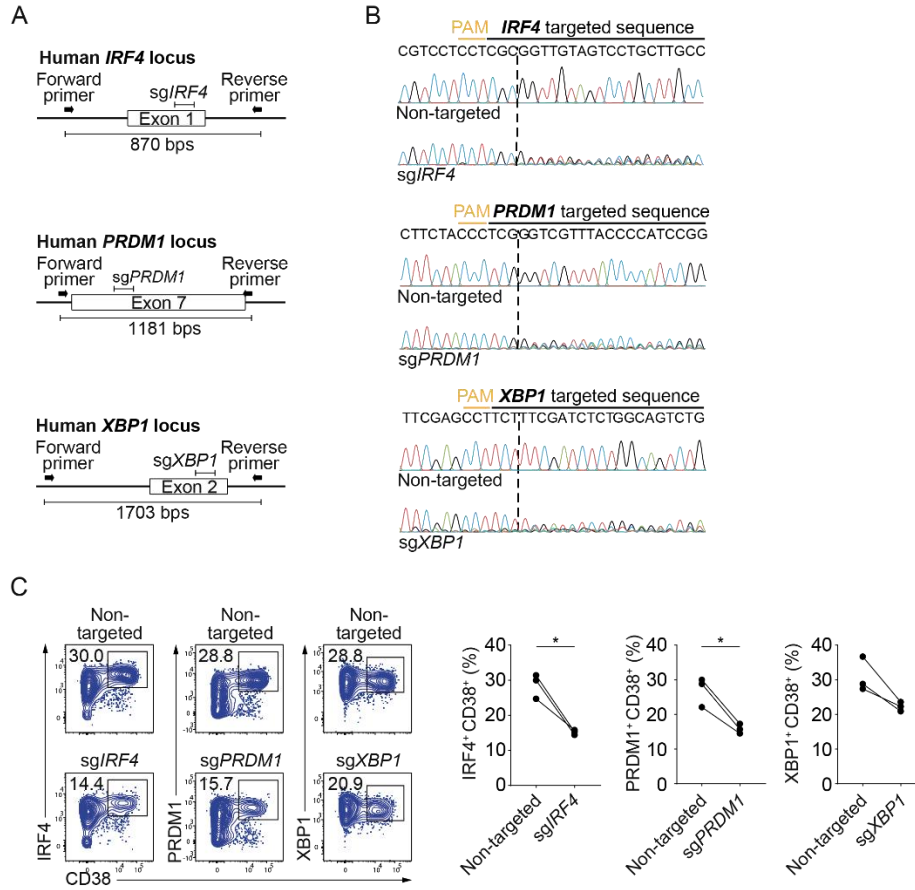
Figure S2: *IRF4*, *PRDM1*, and *XBP1* are crucial for B cell survival and PC differentiation *in vitro*. (A) The schemes show the targeted site of indicated genes and primer sites for amplifying of flanking regions of *IRF4, PRDM1,* and *XBP1*-targeted sites by PCR. (B) Sanger sequencing signal traces show noise peaks at *IRF4, PRDM1,* and *XBP1*-targeted site compared to non-targeted samples, respectively. The dashed lines indicate Cas9 cleavage sites. (C) Representative FACS plots (left) and graphs (right) show the percentage of IRF4⁺CD38⁺ PRDM1⁺CD38⁺ and XBP1⁺CD38⁺ cells at day 8 post transduction from non-targeted compared with corresponding sg*IRF4*, sg*PRDM1*, and *sgXBP1*-targeted samples. IRF4⁺CD38⁺ PRDM1⁺CD38⁺, XBP1⁺CD38⁺ cells were determined based on their isotype control stainings. Data were pooled from 3 donors. Statistical significance was calculated using paired *t*-test, only significant p value is shown: $*p < 0.05$. Each gene was independently targeted by three different sgRNAs. Data for one sgRNA are shown.